Creep Deformation of Polycrystalline Mullite

Yasunori OKAMOTO, Hidetaka FUKUDOME, Kunio HAYASHI
and Tomozo NISHIKAWA

Department of Chemistry and Materials Technology, Kyoto Institute of Technology, Matsugasaki, Sakyo-ku, Kyoto, 606 Japan

Abstract:

Creep tests for polycrystalline mullites ($3Al_2O_3 \cdot 2SiO_2$; the average grain sizes, $\underline{d}$ = 1.4 and 2.1 μm) were carried out in air at temperatures between 1365° and 1480°C. The dependence of steady state strain rates, $\dot{\varepsilon}$, on stress and grain size was given by $\dot{\varepsilon} \propto \sigma/\underline{d}^{2.5}$ at lower temperatures (<1460°C), suggesting the deformation mechanism is diffusional creep. The effective diffusion coefficients were calculated using the rate equation of diffusional creep of mixed oxides, showing very high activation energy (810 kJ/mol). The stress exponent was found to increase not only at higher temperatures but also at stresses just before fracture without apparent tertiary creep. The SEM examination revealed two types of fracture mode: slow crack growth pattern observed on the fracture surface of specimens with small grain size, and cavitation at grain boundaries (intergranular separation) observed on the tensile surface of specimens with larger grain size.

1. Introduction

Dense polycrystalline mullites with a little or no glassy phases have become available by sintering fine mullite powders [1-3], and the mechanical properties, including the creep behavior, of those ceramics have been reported [3-7]. Although mullite polycrystals were shown to have excellent creep resistance at high temperatures, the deformation mechanisms are not completely clarified because of insufficient data on the creep behavior (the dependence of creep rate on grain size, stress and temperature) and on the diffusivity of ions in mullite.

In the present study, bending creep tests were carried out to elucidate the deformation mechanisms. Some data on creep fracture were also obtained in the experiments.

2. Experimental Procedure

The polycrystalline mullite samples were obtained by sintering a fine powder* of nominally stoichiometric mullite ($3Al_2O_3 \cdot Si_2O_3$) at 1650°C for 2 h (sample A). A few of these samples were annealed at 1680°C for 10 h to obtain coarser grained samples (sample B). The average grain sizes of samples A and B were 1.4 and 2.1 μm, respectively (the average linear intercepts multiplied by the factor of 1.5).

---

* Prepared using the sol-gel method by Chichibu Cement Co., Tokyo, Japan. Major impurities are TiO_2 <0.2 wt%, Fe_2O_3 <0.01 wt%, Na_2O and K_2O <0.01. Lattice parameters determined by XRD measurements are: $\underline{a}$= 7.5466, $\underline{b}$= 7.6932 and $\underline{c}$= 2.8847 Å. Samples were sintered by Hitachi Zosen, Corp., Osaka, Japan.

Specimens with average dimensions of 2 by 4.5 by 45 mm were machined, polished, and then chamfered.

Creep tests were carried out in air in four-point bending using fixtures made of dense, coarse-grained alumina, at temperatures between 1365° and 1480°C, and at stresses ranging from 10 to 100 MPa. The major and minor spans were 35 and 11 mm, respectively. After an apparent steady state occurred at an applied load, the load was increased (incremental stress testing). The stress and strain rate were calculated using equations derived by Hollenberg et al [8]. The tensile surfaces and creep-fracture surfaces were examined in a scanning electron microscope (SEM) with attention to grain growth, creep damage (cavitation) and fracture mode.

3. Results

Figure 1 shows the microstructures of samples. Some pores are present at grain boundaries. Apparent glassy phases are not observed. However, traces of a glassy phase at the grain boundaries were reported for a mullite which was sintered using the same powder [7]. Some mechanical properties of sample A are given in Table I. Figure 2 shows the flexural strength as a function of temperature (sample A).

The plots of steady-state strain (creep) rates, $\dot{\varepsilon}$, vs stress, σ, are shown in Fig. 3. The stress exponent, n, was ≈ 1 at lower temperatures, while it increases at higher temperature (>1440°C). It is noted that the strain rates increase at stresses just before creep fracture without apparent tertiary creep regions, resulting in the increase in the value of n. Figure 4 shows the dependence of strain rate on grain size, d, indicating $p \approx 2.5$, where p is the grain size exponent defined

by $\dot{\varepsilon} \propto \sigma^n / d^p$. The temperature dependence of strain rate is shown in Fig. 5, indicating a relatively high activation energy for creep deformation ($\approx$ 870 kJ/mol).

4. Discussion

The results shown in Fig. 3 and 4 suggest that the deformation of both mullite samples is diffusional creep in a large portion of the stress-temperature field tested. In diffusional creep of mullite ($Al_6Si_2O_{13}$), the strain rate is given by [10,11]

$$\dot{\varepsilon} = \frac{14\sigma\Omega_M}{d^2 kT} D_{eff} \qquad (1)$$

where Ω_M is the 'molecular' volume (= 2.23×10^{-22} cm^3 for stoichiometric mullite), k is Boltzmann's constant, T is the temperature and D_{eff} is the effective diffusion coefficient for the 'molecule' $Al_6Si_2O_{13}$:

$$D_{eff} = \frac{1}{(6/D^e_{Al}) + (2/D^e_{Si}) + (13/D^e_{Al})} \qquad (2)$$

where D^e_A is the effective diffusion coefficient of ion A (A = Al, Si and O):

$$D^e_A = D^l_A + (\pi/d)\delta D^b_A \qquad (3)$$

where D^l_A is the lattice diffusion coefficient of A, D^b_A is the boundary

diffusion coefficient of A and δ is the grain-boundary width. Considering the structure of mullite which has a number of oxygen vacancies in the lattice [12], and taking account of the analogy to the structure of forsterite (Mg_2SiO_4) [13], it is inferred that $\underline{D}^l_{Al} > \underline{D}^l_O > D^l_{Si}$. At present, however, we have little information on the diffusion coefficients of ions in mullite, with an exception of the data reported by Aksay et al [14]. The grain-size exponent $\underline{p}(=2.5)$ shown in Fig. 4 suggests that the diffusion of the rate limiting species both through the lattice and along the grain boundaries controls the deformation (Eq. 3); i.e. both Nabarro-Herring creep and Coble creep contribute to the strain rate. Effective diffusion coefficients calculated in diffusional creep region ($\underline{n} \approx 1$) using Eq. 1 are plotted in Fig. 6, where the least-squares fit (solid line) gives the value as $\underline{D}_{eff} = 3.6 \times 10^{10} \exp(-810 \pm 13$ [kJ/mol]/$\underline{RT}$). Diffusivities in mullite [14] and those of Si and O in forsterite [13,15,16] are also plotted for comparison. Note that the activation energy in mullite is very high compared to those for Si and O in forsterite. The apparent activation energies and stress exponents for deformation so far reported are listed in Table II. The high value of activation energy in the present work as well as those reported by Kumazawa et al [18] and Ohira et al [21] is remarkable. These high activation energies are unlikely due to grain-boundary diffusion. Davis and Pask [22] have shown that the diffusion through liquid of the Al_2O_3-SiO_2 system depends on the concentration of Al_2O_3 and shows very high apparent activation energy at low concentrations (e.g., $\approx$ 1300 kJ/mol at 4 wt% Al_2O_3). Furthermore, polycrystals containing glassy phases at grain boundaries deform via pressure solution (solution precipitation), showing high apparent activation energies [23-25]. However, the stress exponents obtained at higher temperatures are higher than

1 (Fig. 3(A)), which implies dislocation creep ($n \geq 3$) or interface-reaction controlled deformation ($n = 2$) rather than solution precipitation ($n = 1$). Further testing especially at higher temperatures as well as the investigation of diffusion of ions through lattice and along grain boundaries in mullite are necessary.

No grain growth during creep testing occurred in both samples. Any cavity formation was not observed on the tensile surface of creep-fractured specimens of sample A (Fig. 7). A little cavitation seen in Fig. 7(A) is not responsible for creep strain. On the fracture surface of sample A, a slow crack growth (SCG) pattern was observed (Fig. 8). Intergranular fracture is predominant in the semielliptical SCG region, while transgranular fracture is predominant in the outside of the region, showing catastrophic fracture. The apparent increase in strain rate prior to creep fracture, which resulted in the apparent increase in stress exponent (Fig. 3), may be induced by slow crack growth. Supposing the SCG region is the origin of catastrophic fracture, though the samples are deformed, the fracture toughness was calculated approximately using the dimensions of the SCG pattern (the controlled surface flaw technique [26]), resulting in an average value of 3.5 $MN/m^{3/2}$ at 1420°C. Apparent fracture toughness appeared to increase at these high temperatures, in spite of the decrease in the strength (see Table I and Fig. 1). Fast-fracture in three-point bending (Fig. 2; elastic strain rate $\approx$ 1.7×10^{-4} s^{-1}) was completely transgranular at these temperatures.

On the other hand, the creep fracture of sample B was completely intergranular as seen in Fig. 8. In addition, many cavities (intergranular separation) were observed on the tensile surface of fractured specimens (Fig. 7(B)), though significant cavitation was not observed for specimens deformed without fracture. These results suggest that the

mechanism of creep fracture in sample B is different from that in sample A: slow crack growth from a fracture origin in sample A, and cavity growth at isolated origins and their coalescence in sample B. However, additional studies of the effect of glassy phases at grain boundaries on deformation and fracture are required for further discussion.

Acknowledgment: The authors thank J. Yano, Hitachi Zosen, Corp., for providing the mullite samples.

References

1. Mazdiyasni, K.S., and Brown, L.M., "Synthesis and Mechanical Properties of Stoichiometric Aluminum Silicate (Mullite)," J. Amer. Ceram. Soc., 55[11], 548-552(1972).

2. Ghate, B.B., Hasselman, D.P.H., and Spriggs, R.M., "Synthesis and Characterization of High Purity, Fine Grained Mullite," Amer. Ceram. Soc. Bull., 52[9], 670-672(1973).

3. Kanzaki, S., Tabata, H., Kumazawa, T., and Ohta, S., "Sintering and Mechanical Properties of Stoichiometric Mullite," J. Amer. Ceram. Soc., 65[1], C-6-C-7(1985).

4. Lessing, P.A., Gordon, R.S., and Mazdiyasni, K.S., "Creep of Polycrystalline Mullite," J. Amer. Ceram. Soc., 58[3-4], 149(1975).

5. Dokko, P.C., Pask, J.A., and Mazdiyasni, K.S., "High-Temperature Mechanical Properties of Mullite Under Compression," J. Amer. Ceram. Soc., 60[3-4], 150-155(1977).

6. Mah, T.-I., and Mazdiyasni, K.S., "Mechanical Properties of Mullite," J. Amer. Ceram. Soc., 66[10], 699-703(1983).

7. Ismail, M.G.M.U., Nakai, Z., and Sōmiya, S., "Microstructure and

Mechanical Properties of Mullite Prepared by the Sol-Gel Method," J. Amer. Ceram. Soc., 70[1], C-7-C-8(1987).

8. Hollenberg, G.W., Terwilliger, G.R., and Gordon, R.S., "Calculation of Stresses and Strains in Four-Point Bending Creep Tests," J. Amer. Ceram. Soc., 54[4], 196-199(1971).

9. Marshall, D.B., and Evans, A.G., "Reply to 'Comment on "Elastic/Plastic Indentation Damage in Ceramics: The Median/Radial Crack System"'," J. Amer. Ceram. Soc., 64[12], C-182-C-183(1981).

10. Gordon, R.S., "Ambipolar Diffusion and its Application to Diffusion Creep," pp. 445-464 in Mass Transport Phenomena in Ceramics (Materials Science Research, vol.9), ed. A.R. Cooper and A.H. Heuer, Plenum Press, New York(1975).

11. Cannon, R.M., and Coble, R.L., "Review of Diffusional Creep of Al_2O_3," pp. 61-99 in Deformation of Ceramic Materials, ed. R.C. Bradt and R.E. Tressler, Plenum Press, New York(1975)

12. Cameron, W.E., "Mullite: A Substituted Alumina," Amer. Mineral., 62, 747-755(1977).

13. Kohlstedt, D.L., and Ricoult, D.L., "High-Temperature Creep of Silicate Olivines," pp. 251-280 in Deformation of Ceramic Materials II (Materials Science Research, vol.18), ed. R.E. Tressler and R.C. Bradt, Plenum Press, New York(1984).

14. Aksay, I.A., Davis, R.F., and Pask, J.A., "Diffusion in Mullite," (abstract) Amer. Ceram. Soc. Bull., 52[9], 710(1973).

15. Ando, K., Kurokawa, H., Oishi, Y., and Takei, H., "Self-Diffusion Coefficient of Oxygen in Single-Crystal Forsterite," J. Amer. Ceram. Soc., 64[2], C-30(1981).

16. Jaoul, O., Poumellec, M., Froidevaux, C., and Havette, A., "Silicon Diffusion in Forsterite," pp. 95-100 in Anelasticity in the Earth, ed.

F.D. Stacey, M.S. Paterson, and A. Nicolas, Amer. Geophys. Union and Geol. Soc. Amer., Washington and Boulder(1981).

17. Penty, R.A., Hasselman, D.P.H., and Spriggs, R.M., "Pressure Sintering Kinetics of Fine Grained Mullite by the Change in Pressure and Temperature Technique," Amer. Ceram. Soc. Bull., 52[9], 692-693(1973).

18. Kumazawa, T., Kanzaki, S., Wakai, F., and Tabata, H., p. 206 in Proceedings of Basic Science Divisional Meeting of the Ceramic Society of Japan(1987).

19. Tomatsu, H., Maeda, K., Ohnishi, H., and Kawanami, T., pp. 51-52 in Proceedings of Annual Meeting of the Ceramic Society of Japan(1987).

20. Ashizuka, M., Okuno, T., and Kubota, Y., p. 173 in Proceedings of Annual Meeting of the Ceramic Society of Japan(1987).

21. Ohira, H., Shiga, H., Ismail, M.G.M.U., Nakai, Z., Akiba, T., and Yasuda, E., p. 12 in Proceedings of Annual Meeting of the Ceramic Society of Japan(1989).

22. Davis, R.F., and Pask, J.A., "Diffusion and Reaction Studies in the System Al_2O_3-SiO_2," J. Amer. Ceram. Soc., 55[10], 525-531(1972).

23. Wan, J.-G., and Raj, R., "Mechanism of Superplastic Flow in a Fine-Grained Ceramic Containing Some Liquid Phase," J. Amer. Ceram. Soc., 67[6], 399-409(1984).

24. Wiederhorn, S.M., Hockey, B.J., Krause, Jr., R.F., and Jakus, K., "Creep and Fracture of a Vitreous-Bonded Aluminium Oxide," J. Mater. Sci., 21, 810-824(1986).

25. Okamoto, Y., Nishi, T., Nishida, T., Hayashi, K., and Nishikawa, T., "Creep and Creep Cavitation in Polycrystalline MgO: Effect of Intergranular Second Phase," pp. 825-830 in Sintering '87 :Proceedings of the 4th International Symposium on Science and Technology of Sintering (Tokyo), ed. S. Sōmiya, M. Shimada, M. Yoshimura and R. Watanabe,

Elsevier Applied Science, London/New York/Tokyo (1988).

26. Petrovic, J.J., Jacobson, L.A., Talty, P.K., and Vesudevan, A.K., "Controlled Surface Flaws in Hot-Pressed Si_3N_4," J. Amer. Ceram. Soc., 58[3-4], 113-116(1975).

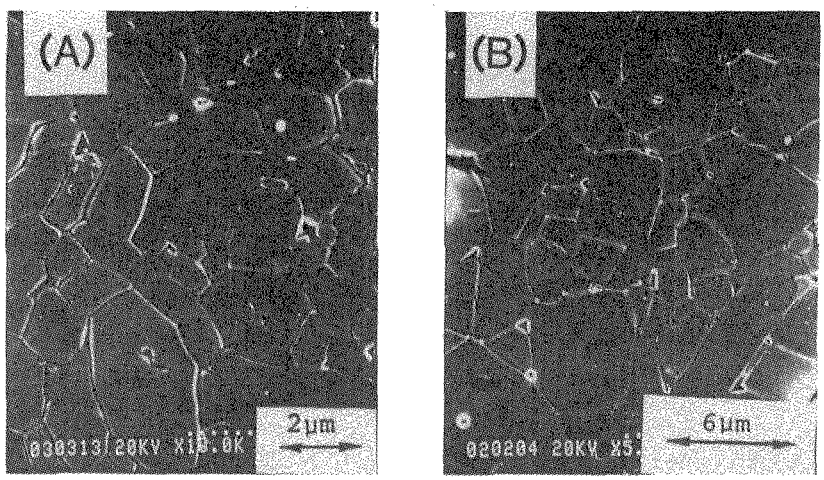

Fig. 1. Microstructures of mullite samples A and B, thermally etched after polishing.

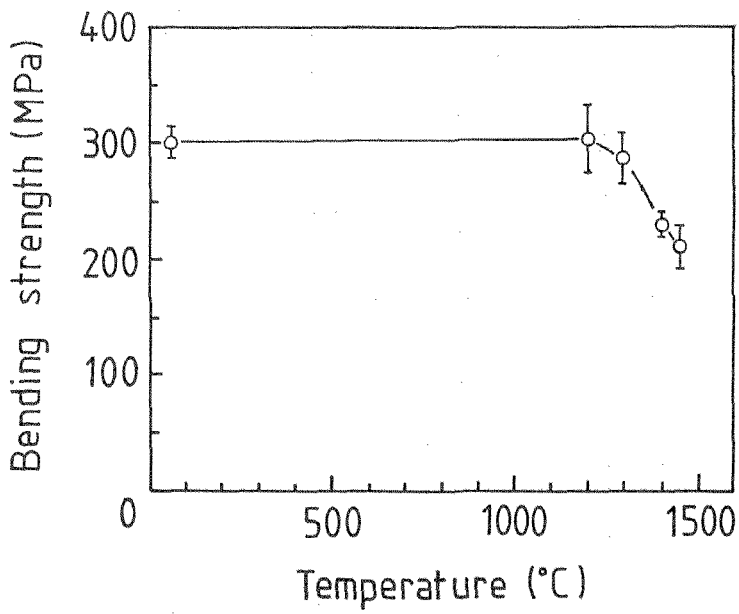

Fig. 2. Flexural strength as a function of temperature for sample A, tested in three-point bending (span = 30 mm).

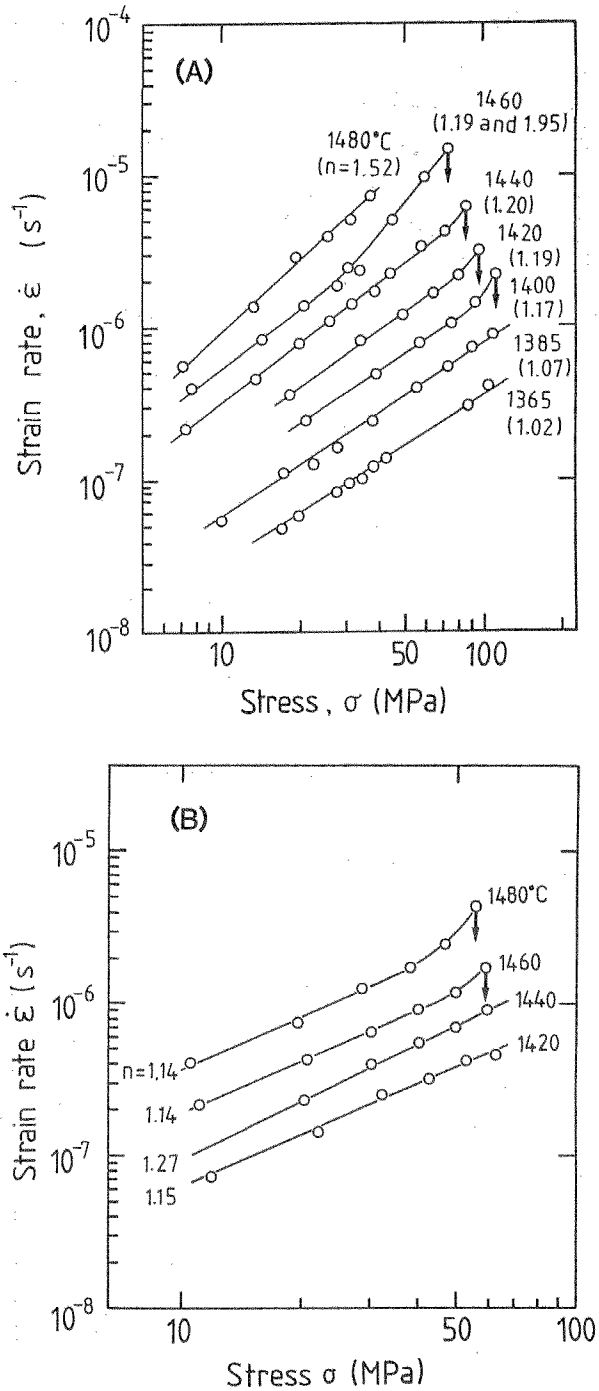

Fig. 3. Steady-state strain rate vs stress for (A) sample A and (B) sample B. The arrows indicate the stresses at which the specimens fractured during creep testing.

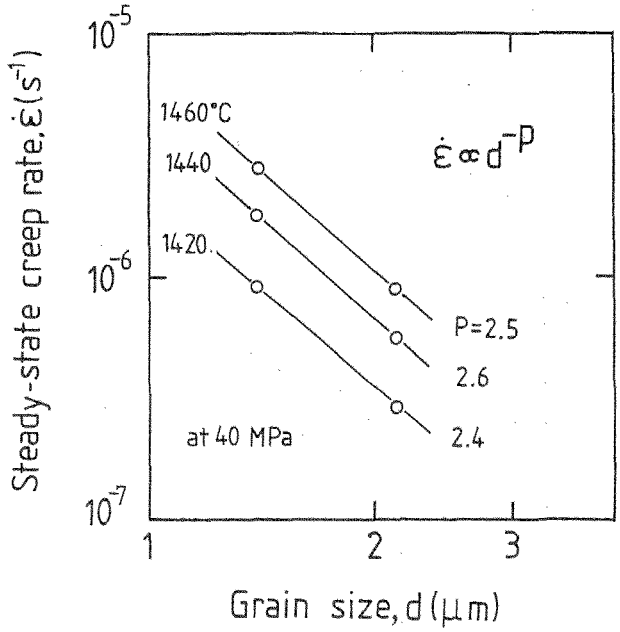

Fig. 4. Effect of grain size on strain rate for creep of mullite.

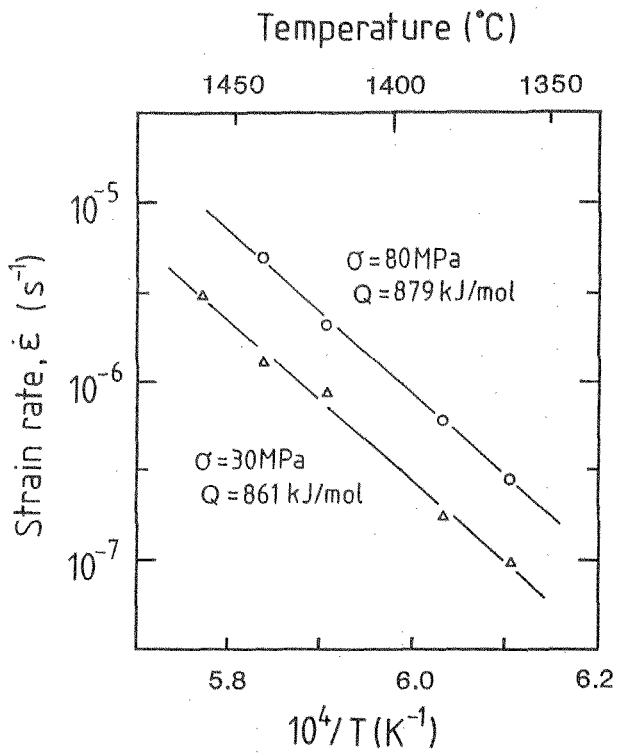

Fig. 5. Temperature dependence of strain rate for mullite (sample A).

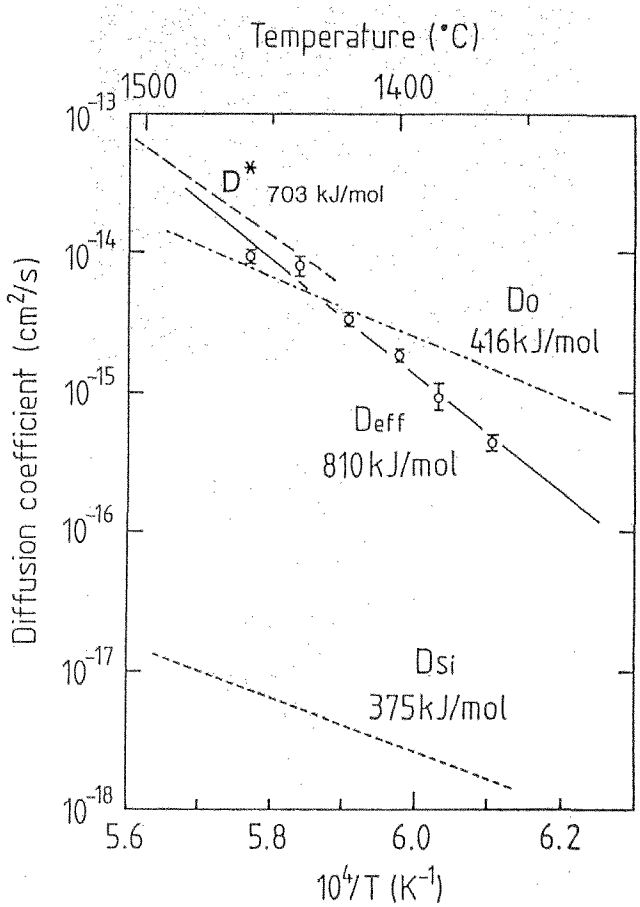

Fig. 6. Effective diffusion coefficients (D_{eff}) calculated from creep strain rates using Eq. 1. D_O and D_{Si} are diffusion coefficients of O [13,15] and Si [13,16], respectively, in forsterite. D^* is diffusion coefficients in mullite [14]. Activation energies are specified on the figure.

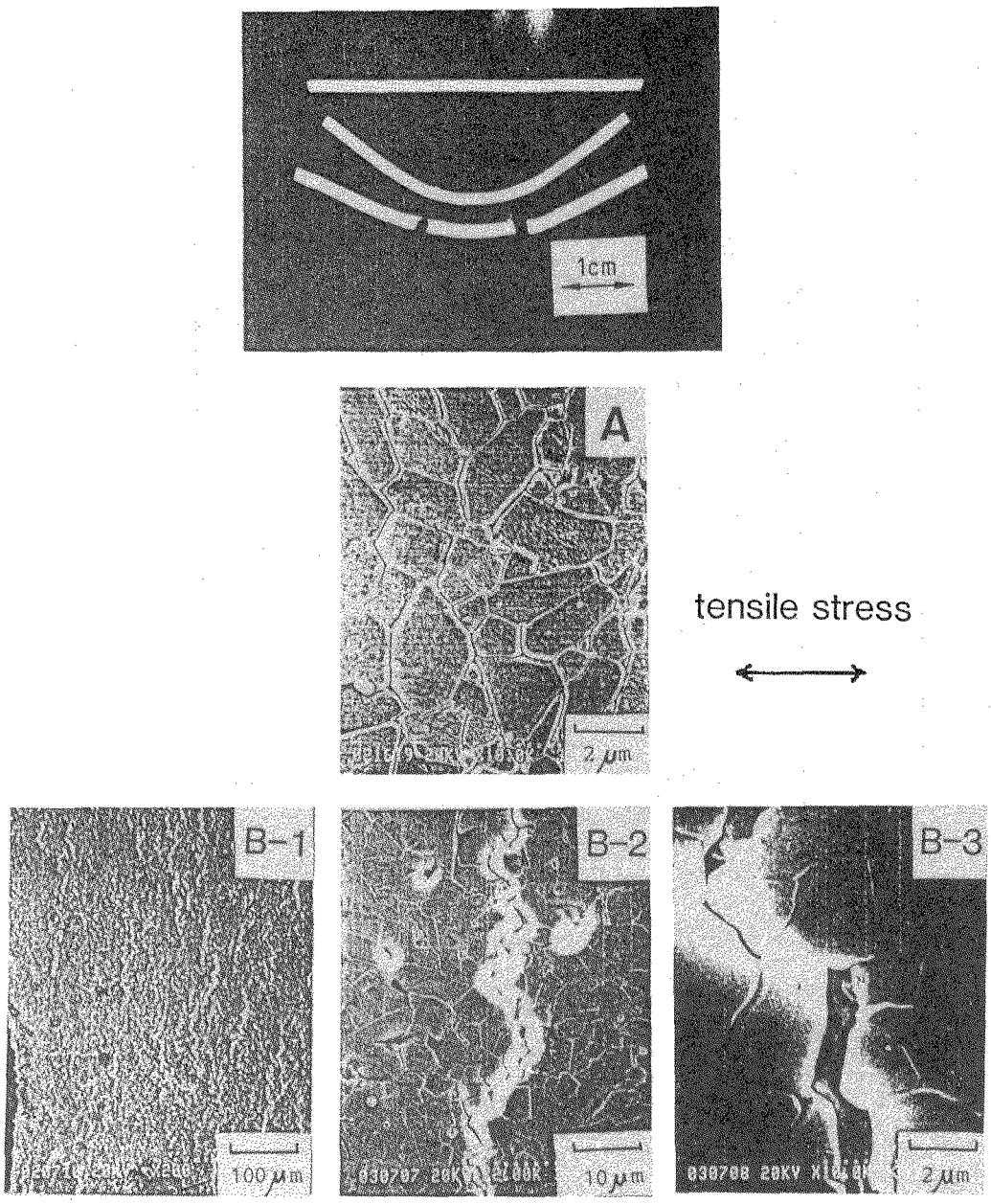

Fig. 7. Deformed and fractured samples and scanning electron micro graphs of tensile surfaces of creep-fractured mullite for (A) sample A tested at 1460°C, 86 MPa; ε = 2.8 %, and (B) sample B tested at 1480°C, 56 MPa; ε = 3.9 %. Significant cavitation is observed on the tensile surface of sample B (B-1 to B-3).

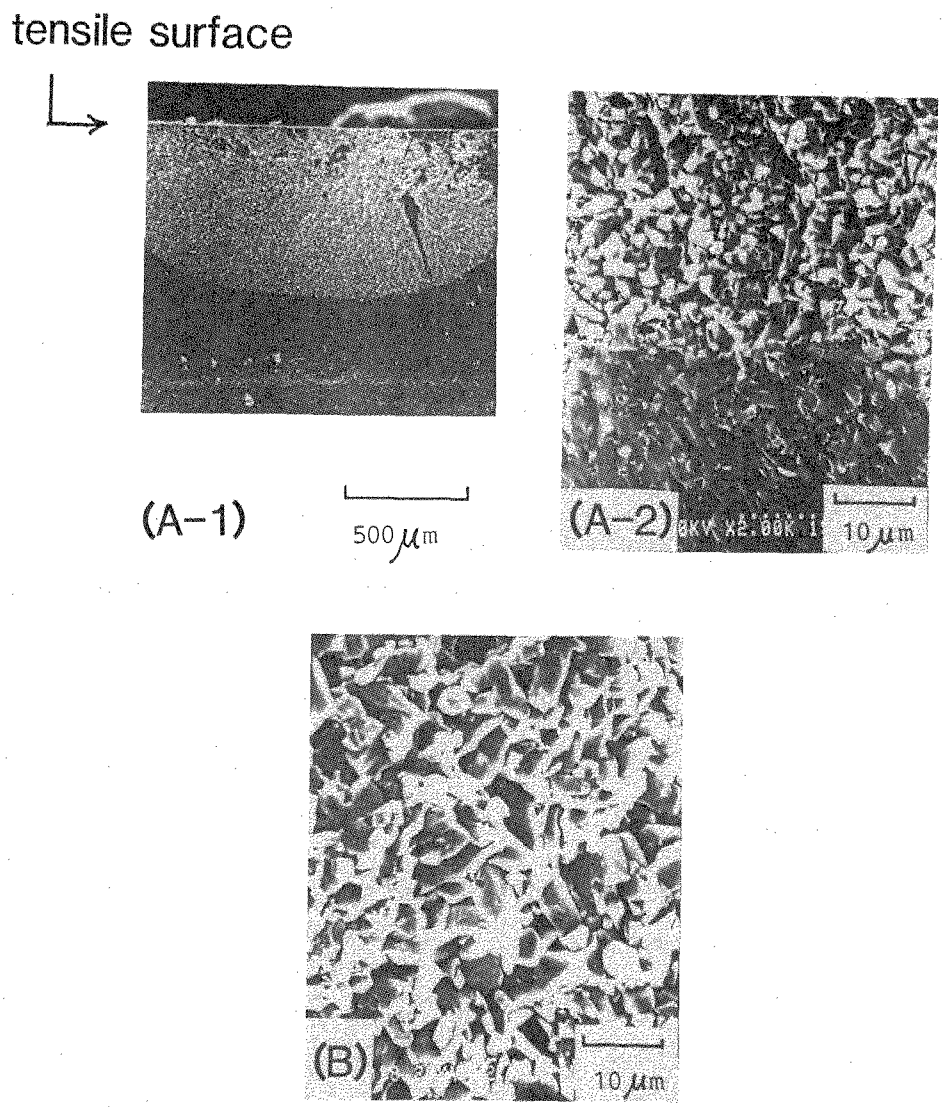

Fig. 8. Scanning electron micrographs of fracture surfaces. (A-1) Sample A tested at 1400°C and 113 MPa ($\dot{\varepsilon}$ = 2.6 %), showing slow crack growth. (A-2) Boundary region between SCG fracture and catastrophic, transgranular fracture. (B) Sample B tested at 1480°C and 56 MPa ($\dot{\varepsilon}$ = 3.9 %), showing intergranular fracture on the whole fracture surface.

Table I. Some mechanical properties of sample A.

Density	(% theoretical)	>98
Young's modulus, E	(GPa)*	224
Flexural strength, σ_f	(MPa)	301 ± 17
Vickers hardness, H_v	(GPa)	10.2 ± 0.4
Fracture toughness, K_{IC}	($MN/m^{3/2}$)**	2.7 ± 0.1

* Flexural resonance technique.

** Indentation fracture method. $K_{IC} = 0.036E^{0.4}P^{0.6}a^{-0.7}(c/a)^{-1.5}$, where P is the indentation load, a is the impression radius and c is the radial crack length [9].

Table II. Stress exponent and activation energy for creep deformation of mullite

Testing	Temperature (°C)	n	Q (kJ/mol)	Reference
Hot pressing	1450–1650	1.4	707	Penty et al [17]
Bending	1350–1450	1.0	687	Lessing et al [4]
Compression	1400–1500	1.0	710	Dokko et al [5]
Tension	1350–1450	1.6	900	Kumazawa et al[18]
Bending	1400–1500	1.3	–	Ohnishi et al [19]
Bending	1400–1500	1.4	703	Ashizuka et al[20]
Compression	1400–1550	1.3	1030	Ohira et al [21]
Bending	1365–1480	1.0	810*	Present study

* Q in D_{eff}.